Apoptotic pore formation is associated with in-plane insertion of Bak or Bax central helices into the mitochondrial outer membrane

Dana Westphal[a,b], Grant Dewson[b,c], Marie Menard[a,1], Paul Frederick[a], Sweta Iyer[a,b], Ray Bartolo[a], Leonie Gibson[a], Peter E. Czabotar[b,d], Brian J. Smith[e], Jerry M. Adams[a,b,2,3], and Ruth M. Kluck[a,b,2,3]

[a]Molecular Genetics of Cancer Division, [c]Cell Signalling and Cell Death Division, and [d]Structural Biology Division, The Walter and Eliza Hall Institute of Medical Research, Parkville, VIC 3052, Australia; [b]Department of Medical Biology, University of Melbourne, Parkville, VIC 3010, Australia; and [e]School of Molecular Sciences, La Trobe Institute for Molecular Sciences, La Trobe University, Melbourne, VIC 3086, Australia

Contributed by Jerry M. Adams, August 15, 2014 (sent for review June 22, 2014)

The pivotal step on the mitochondrial pathway to apoptosis is permeabilization of the mitochondrial outer membrane (MOM) by oligomers of the B-cell lymphoma-2 (Bcl-2) family members Bak or Bax. However, how they disrupt MOM integrity is unknown. A longstanding model is that activated Bak and Bax insert two α-helices, α5 and α6, as a hairpin across the MOM, but recent insights on the oligomer structures question this model. We have clarified how these helices contribute to MOM perforation by determining that, in the oligomers, Bak α5 (like Bax α5) remains part of the protein core and that a membrane-impermeable cysteine reagent can label cysteines placed at many positions in α5 and α6 of both Bak and Bax. The results are inconsistent with the hairpin insertion model but support an in-plane model in which α5 and α6 collapse onto the membrane and insert shallowly to drive formation of proteolipidic pores.

cell death | mitochondrial permeabilization | protein-membrane topology | membrane pores | cysteine-scanning mutagenesis

Commitment of cells to apoptosis is determined primarily by interactions within the B-cell lymphoma-2 (Bcl-2) protein family on the mitochondrial outer membrane (MOM) (1–4). The proapoptotic members Bcl-2 antagonist/killer (Bak) and Bcl-2–associated X protein (Bax) mediate the pivotal step of MOM permeabilization, which releases proteins, such as cytochrome c, that promote the proteolytic demolition by caspases. Two other Bcl-2 subfamilies tightly control Bak and Bax activation. Their activation is promoted by the Bcl-2 homology domain 3 (BH3)-only proteins, such as BH3-interacting domain death agonist (Bid), the truncated form of which (tBid) can directly bind both. Conversely, prosurvival family members can bind and inhibit activated Bak and Bax, as well as the BH3-only proteins.

Like their prosurvival relatives, Bak and Bax in healthy cells are globular monomers, comprising similar helical bundles with a hydrophobic α-helix (α5) surrounded by amphipathic helices (5, 6). Their C-terminal helix (α9) is a hydrophobic transmembrane (TM) domain that anchors them in the MOM. In healthy cells Bak is already anchored there, presumably solely by α9, whereas Bax is primarily cytosolic (5), accumulating at the MOM after an apoptotic signal and inserting its α9. Other major conformational changes in both Bak and Bax, reviewed in ref 4, include exposure of their BH3 (α2) and its reburial within the surface groove of another activated Bak or Bax molecule (7–10). These novel "symmetric" homo-dimers can multimerize via association of α6 helices (8, 11, 12).

Although oligomeric Bak and Bax are highly implicated in MOM permeabilization, how they interact with the membrane to form pores remains a mystery. The first structure of a Bcl-2 family member, the prosurvival protein Bcl-x_L (13), and later those of Bax (5) and Bak (6), provided a tantalizing clue: similarities with the pore-forming domains of bacterial toxins, such as diphtheria toxin or colicin A. To form pores, these toxins are thought to insert their two hydrophobic core helices as a hairpin across the membrane (14), suggesting that the central helices of Bak and Bax (α5 and α6) might penetrate the MOM similarly (reviewed in refs 3, 15, and 16). Consistent with this hairpin insertion model, α5 and α6 peptides can permeabilize membranes (17–19). More pertinently, Bax α5 and α6 were reported to insert into and span the MOM as a hairpin before oligomerization (20).

This longstanding model, however, does not fit well with recent evidence on the structure of Bak and Bax oligomers, as recently reviewed (2, 4). Analysis of Bak oligomers in liposomes by electron paramagnetic resonance (EPR) suggests that α6 inserts only shallowly in the lipid bilayer (21). Additionaly, the first 3D structures of activated forms of Bax (10) suggest that, early in its activation, α5 and α6 separate. Moreover, a Bax core domain containing only helices α2 to α5 generated a BH3:groove symmetric dimer in which two α4 and two α5 helices form an aromatic face that might sit on the bilayer (10). These findings fit better with an "in-plane model" in which only α9 is a TM domain and other helices (including α5 and α6) insert only shallowly into the bilayer.

The nature of the apoptotic pores remains uncertain. Some findings favor a proteinaceous pore (22), but studies with model membranes suggest that Bax oligomers can perturb the bilayer and produce lipidic pores (i.e., pores not bounded entirely by protein) (23–26).

Significance

To trigger cell death (apoptosis), two members of the B-cell lymphoma-2 protein family, Bak and Bax, change shape and convert from inert monomers into the oligomers that disrupt the outer mitochondrial membrane, but how they perturb the membrane is poorly understood. A longstanding model is that they rearrange and insert two central helices, α5 and α6, as a hairpin through the membrane. We show, however, that the hairpin insertion model does not hold. Instead, these helices in the oligomers insert only shallowly in the membrane, in its plane. The results favor a model in which these and probably other helices of Bak and Bax crowd the outer leaflet of the membrane, producing membrane curvature that leads to its disruption.

Author contributions: D.W., G.D., J.M.A., and R.M.K. designed research; D.W., G.D., M.M., P.F., S.I., R.B., L.G., and B.J.S. performed research; D.W., G.D., M.M., P.E.C., B.J.S., J.M.A., and R.M.K. analyzed data; and D.W., J.M.A., and R.M.K. wrote the paper.

The authors declare no conflict of interest.

Freely available online through the PNAS open access option.

[1]Present address: Apoptosis, Cancer and Development Laboratory, Centre de Cancérologie de Lyon, Université de Lyon, 69008 Lyon, France.

[2]J.M.A. and R.M.K. contributed equally to this work.

[3]To whom correspondence may be addressed. Email: adams@wehi.edu.au or kluck@wehi.edu.au.

This article contains supporting information online at www.pnas.org/lookup/suppl/doi:10.1073/pnas.1415142111/-/DCSupplemental.

These important unresolved questions about the pivotal event in apoptosis prompted us to explore the membrane topology of Bak, before, during, and after an apoptotic signal, and to reinvestigate that of Bax. In accord with recent Bax structures (10) and recent EPR studies on Bak (21, 27), the results show that neither oligomeric Bak nor Bax inserts an α5–α6 hairpin across the MOM. We propose instead that the α5 and α6 helices lie in the bilayer plane and disrupt membrane integrity by imposing tension and curvature to the membrane that provoke its permeabilization.

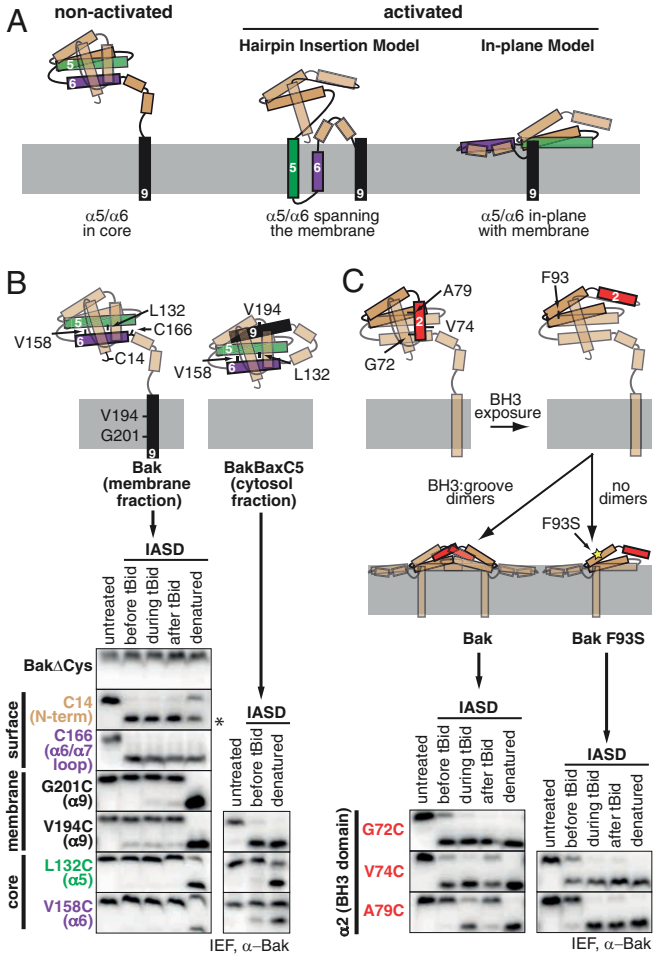

Fig. 1. Models of Bak membrane topology and the cysteine accessibility approach. (*A*) Two models of Bak membrane topology following its activation. Nonactivated Bak is anchored via α9 and the α5/α6 hairpin is in the protein interior. Upon activation, in the hairpin insertion model, the α5/α6 hairpin inserts to span the MOM, whereas in an in-plane model, α6 disengages from the core (α2–α5), allowing both α5 and α6 to lie in-plane on the membrane surface. (*B*) IASD labeling is reduced for cysteines within the Bak hydrophobic core or the MOM. Bak or a semicytosolic mutant BakBaxC5 with cysteines at the indicated positions was stably expressed in $Bak^{-/-}Bax^{-/-}$ MEFs. Membrane fractions (*Left*) were incubated with tBid or denatured with the detergent ASB-16, and labeled with IASD. Cytosol fractions (*Right*) were treated similarly, but not incubated with tBid. To resolve IASD-labeled and unlabeled Bak, samples were solubilized and run on IEF gels, followed by blotting for Bak. Cysteine location is color-coded (α5, green; α6, purple; α9, black). The asterisk denotes IASD-labeled Bak. Data are representative of two or more independent experiments. Fig. S2*A* gives percent exposure of these cysteines to IASD. (*C*) Cysteines in the BH3:groove dimer interface are refractory to IASD labeling. Cysteines were placed in α2 of Bak or the F93S loss-of-function variant (yellow star), which is activated by tBid but fails to dimerize (Fig. S2*F*). Membrane fractions were processed as in *B*. Data are representative of two or more independent experiments.

Results

Fig. 1*A* depicts two models for the membrane topology of activated Bak. In the hairpin insertion model proposed for Bax (20), α5 and α6 dissociate from the protein core and penetrate the MOM as a hairpin, creating a multipass membrane protein. However, if instead α6 dissociates from α5 while α5 remains part of the protein α2–α5 core, as crystal structures for activated Bax suggest (10), both α5 and α6 might insert only one helical face into the lipid bilayer, as in the in-plane model shown.

To distinguish these models, we have explored Bak membrane topology by a cysteine-accessibility approach similar to that used with Bax (20). Single cysteines were substituted at 30 positions in cysteine-null Bak (BakΔCys; i.e., C14S/C166S), and each mutant stably expressed in $Bak^{-/-}Bax^{-/-}$ mouse embryonic fibroblasts (MEFs) and tested for function; nearly all remained active (Fig. S1 and Tables S1 and S2). To trigger Bak activation, we then incubated mitochondrial fractions with tBid, which converts nearly all of Bak to the active oligomers (7), and treated them with the thiol-specific labeling reagent 4-acetamido-4'-((iodoacetyl) amino)stilbene-2,2'-disulfonic acid (IASD). Its two negative sulfonate charges prevent IASD from accessing cysteines in hydrophobic environments, such as the MOM, and allow isoelectric focusing (IEF) to resolve IASD-labeled and unlabeled Bak (Fig. 1*B*). As well as a control not exposed to IASD and another fully exposed to labeling by denaturation and membrane solubilization, each cysteine-substituted Bak variant was routinely assessed for labeling before, during, or after tBid incubation (Fig. 1*B*). The approach thus monitors exposure of the residue in both monomeric nonactivated Bak (the "before tBid" sample) and fully oligomeric Bak after tBid treatment, whereas the labeling "during tBid" treatment was designed to also detect transient exposure of the residue during Bak activation.

Cysteines in the Protein Interior and Protein Interfaces as Well as the Membrane Resist IASD Labeling. As expected, BakΔCys remained unlabeled, whereas surface residues (C14 and C166) were fully labeled before, during, and after tBid treatment, and α9 substitutions (V194C and G201C) remained unlabeled, consistent with their burial in the MOM (Fig. 1*B*, *Left*, and Fig. S2*A*). We confirmed that only α9 anchors nonactivated Bak in the MOM by showing that cleavage at a unique protease site placed in the α8–α9 loop released truncated Bak into the cytosol (Fig. S2 *B–D*). Whether α9 remains the sole membrane anchor in activated Bak was indeterminable because that site became refractory to cleavage (Fig. S2*D*, lane 8).

Notably, cysteines in the Bak hydrophobic interior (L132 and V158) were also unlabeled, both in mitochondrial Bak (Fig. 1*B*, *Left*) and the semicytosolic mutant BakBaxC5 (28) (Fig. 1*B*, *Right*, and Fig. S2*A*). Thus, cysteines buried in either the MOM or the hydrophobic protein interior remained unlabeled, as generally observed (29).

We demonstrated that IASD also did not label cysteines within the BH3:groove interface of Bak dimers (Fig. 1*C* and Fig. S2*A*), using substitutions in the Bak BH3 (α2). The hydrophobic side of that helix faces the protein interior before apoptosis, but is transiently exposed by an apoptotic stimulus before it binds into the groove of another Bak molecule (7). BH3 residues V74C and A79C orient toward the protein core (Fig. S2*E*) in both the structure of nonactivated Bak and a homology model of the Bak BH3:groove (α2–α5) dimer, based on the Bax α2–α5 dimer structure (10). Both residues consistently labeled most during tBid incubation (Fig. 1*C*, *Left*), indicating transient exposure. Moreover, if Bak also contained a loss-of-function mutation (F93S) that allows BH3 release but not Bak dimerization (12) (Figs. S1*A* and S2*F*), both V74C and A79C stayed entirely exposed after tBid treatment (Fig. 1*C*, *Right*).

Thus, cysteine accessibility distinguishes Bak residues on the protein surface from those buried in the MOM, the protein interior, or a protein–protein interface, and detects transient conformation changes.

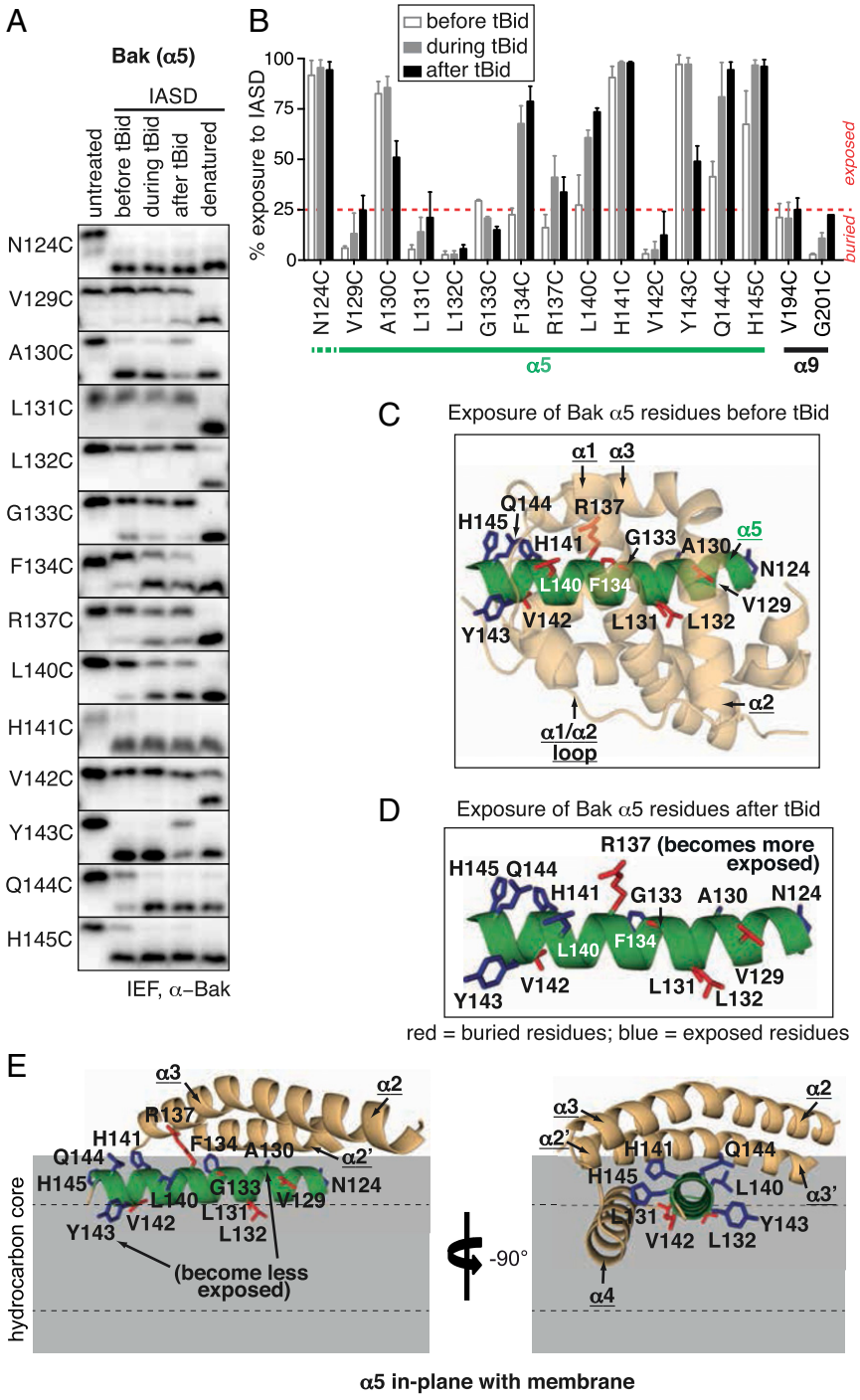

Fig. 2. Many α5 residues in oligomeric Bak are at least partly exposed to IASD. (*A*) IASD labeling of Bak α5 residues before, during and after tBid, processed, as in Fig. 1*B*. Data are representative of two or more independent experiments. Bak F134C, a loss-of-function variant, exposes its BH3 domain after tBid but fails to dimerize (Fig. S3*C*). (*B*) Quantified IASD labeling of α5. A red broken line indicates the distinction between "exposed" and "buried," based on the ~25% labeling of central cysteines in the TM domain (α9). Data are mean ± SD (n = 3) or range (n = 2 for G133C, H141C, H145C, G201C). (*C* and *D*) The α5 central region is buried before and after tBid, whereas its C-terminal segment shows increased sidedness. The structure of nonactivated Bak (PDB ID code 2IMT) shows the location of residues that are exposed (blue) or buried (red) either before (*C*) or after tBid treatment (*D*), based on statistically significant difference ($P < 0.05$) with the α9 residue V194C. See also Fig. S3. Notably, R137 was labeled significantly more after than before tBid exposure ($P < 0.04$). (*E*) Model of Bak α5 in-plane with the MOM. A homology model of a Bak BH3:groove dimer, based on the α2–α5 Bax dimer structure (10) (PDB ID code 4BDU) shows α5 remaining with the protein core (α2–α5); α5 presents one face to the membrane but contacts α2 and α3 above, as well as α4 on one side and the second dimer α5 chain on the other side (not shown). Some helices have been omitted for clarity. The hydrocarbon core of the membrane (gray) is ~30 Å thick, and dotted lines indicate the depth (7.5 Å) to which IASD may penetrate from each side of the membrane (31). The depth to which α4 sinks in the membrane is uncertain, because in the homology model, like the Bax crystal structure (10), there is an angle between the two α4–α5 hairpins, but contact with the membrane may well promote a flatter protein surface.

In Oligomeric Bak, α5 Is a Vital Core Constituent Rather than a TM Domain. To identify Bak α5 residues in an aqueous environment, we tested the 12 functional cysteine replacements (Fig. S1 and Table S1) for IASD labeling (Fig. 2 *A* and *B*). We judged them to be exposed if their labeling was significantly greater than the ~25% found with two central α9 residues (V194C and G201C) (Fig. 2*B*). To help interpret tBid-induced changes, we plotted labeling before tBid against that after tBid, revealing four patterns: always buried, always exposed, become more exposed, or become less exposed (Fig. S3*A*).

The IASD labeling of α5 before tBid (i.e., with no tBid treatment) is consistent with the nonactivated Bak structure (PDB ID code 2IMT) (Fig. 2*C*): residues near both ends of α5 were exposed (Fig. 2*C*, blue), whereas those in the middle were buried (Fig. 2*C*, red). Labeling after tBid also showed a trend for exposed residues toward the helix ends and continued burial of central residues (Fig. 2*D*), although in the C-terminal part of α5, Y143 consistently labeled less and L140C and Q144C consistently labeled more (Fig. 2*B*).

TM domains treated with cysteine probes like IASD typically display a central span of 10–12 unlabeled residues across the center of the membrane (30, 31). A span of up to nine residues (flanked by A130C and L140C) might be buried in activated Bak α5 (Fig. 2 *A*, *B*, and *D*), because three residues (L131C, L132C, G133C) within this stretch were clearly buried after tBid treatment, and the 34% labeling of R137C was not significantly above

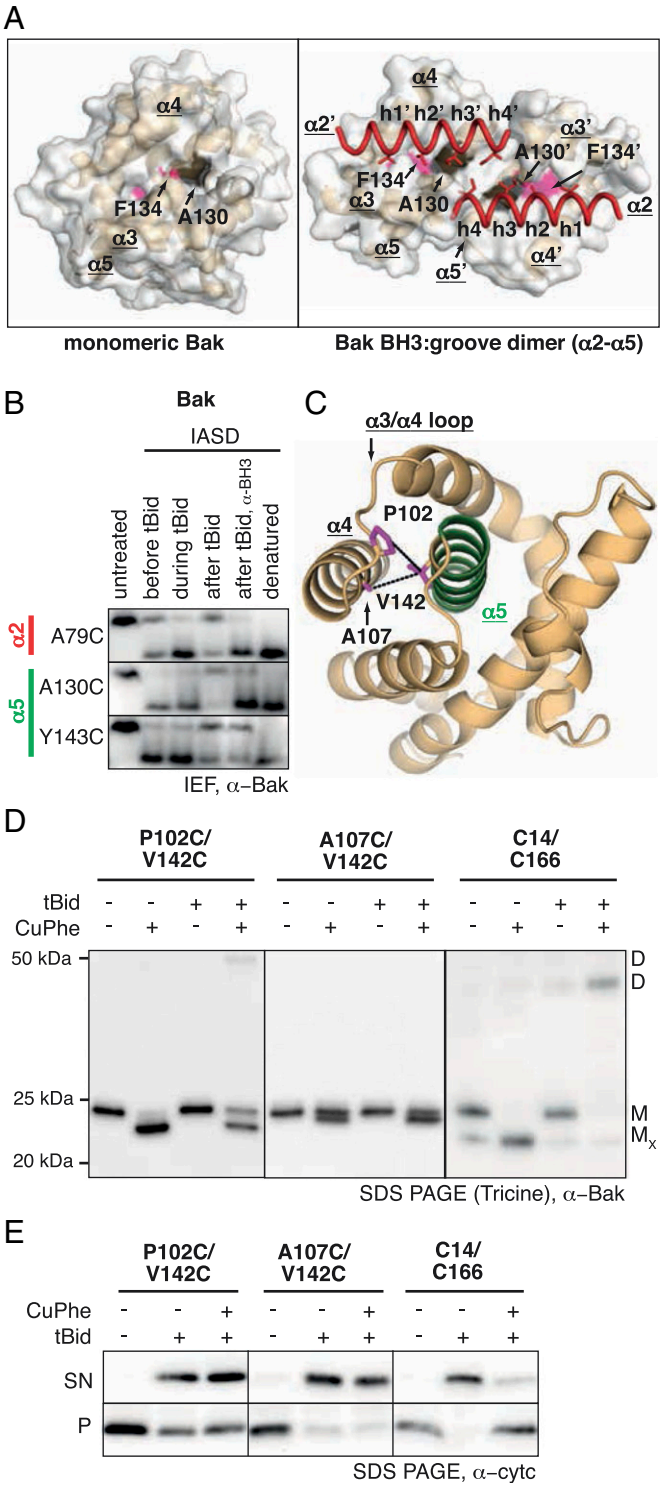

Fig. 3. In activated Bak, central α5 residues remain within the protein core. (*A*) A central region of Bak α5, including A130 and F134, contributes to the BH3-binding groove, which is required for Bak oligomerization. A130 (black) and F134 (pink) are indicated on monomeric Bak (*Left*, PDB ID code 2M5B with Bid SAHBa peptide removed) (36) and a homology model of the Bak BH3:groove dimer (*Right*), showing the two α2 helices (red tubes) and the BH3 h1-h4 residues (red side-chains), which make key hydrophobic contacts in the groove. A130 and F134 probably would be occluded in nonactivated Bak by a bound Bid BH3 peptide (not shown), as they are by Bak α2 in the Bak α2–α5 dimer. (*B*) The α5 residue A130 remains exposed if Bak dimerization is blocked. Mitochondrial membranes were processed as in Fig. 2*A*, but with an α-BH3 antibody (5 μg) added during tBid treatment in lane 5, or just before IEF in other lanes. Data are representative of two independent experiments. Whereas A130C (like A79C) remained exposed in the presence of the antibody, Y143C became less exposed, suggesting that α5 collapses onto the MOM before Bak dimerization. (*C–E*) Tethering evidence that α5 remains with the protein core. (*C*) The disulfide tethers between α5 (V142C) and the α3/α4 loop (P102C) or α4 (A107C) are shown (magenta). (*D*) Long SDS/PAGE runs confirm that oxidation converts the Bak mutants (M) to the expected disulfide-bonded monomers (M_x), whereas wld-type Bak (C14/C166) instead forms a disulfide-linked dimer (D). Data are representative of three independent experiments. (*E*) Tethering Bak α5 to the α2–α4 core does not block cytochrome *c* release. Where indicated, the oxidant CuPhe was added before tBid. Supernatant (SN) and pellet (P) fractions were blotted for cytochrome *c*. Data are representative of three independent experiments.

that of the α9 residues ($P = 0.2$). Unfortunately, the remaining five residues within this stretch were not informative, because of loss-of-function or failure to label even after denaturation (Table S1). Although this nine-residue stretch in Bak α5 might seem compatible with a TM domain, as in the hairpin insertion model (Fig. S3*B*), several considerations make that very unlikely.

First, the C-terminal portion of a TM helix should be fully exposed to IASD (30, 31). In contrast, that portion of α5 labeled periodically after tBid treatment; that is, the last six residues alternated abruptly from exposure (L140C/H141C) to full/partial burial (V142C/Y143C) and then exposure again (Q144C/H145C) (Fig. 2 *A*, *B*, and *D*). This pattern favors an in-plane model (Fig. 2*E*), because side-chain immersion alternates along an in-plane helix. The partial burial of Y143C suggests shallow immersion in the outer leaflet of the bilayer (Fig. 2*E*).

Second, the IASD data indicate that central Bak α5 residues, including A130 and F134, remain part of the BH3-binding groove in oligomeric Bak. A130 and F134 line that groove not only in nonactivated Bak (PDB ID code 2M5B) (Fig. 3*A*, *Left*) but also in the homology model of the Bak BH3:groove α2–α5 dimer, where the BH3 (α2) helices occlude A130 and F134 (Fig. 3*A*, *Right*). Accordingly, A130C became less exposed to IASD after tBid (Fig. 3*B*), but remained exposed if an antibody to the Bak BH3 domain precluded Bak dimerization (Fig. 3*B*, lane 5), consistent with the Bak BH3 blocking this face of α5 in oligomeric Bak (Fig. 3*A*, *Right*). Although Bak F134C had lost function (Fig. S1*A*), it was stably expressed and changed conformation after tBid but did not dimerize (Fig. S3*C*). Accordingly, F134C became more exposed after tBid (Fig. 2 *A* and *B*), suggesting the groove opens but cannot then be filled by the Bak BH3 domain.

Third, whereas α5 and α6 leave the protein core in the hairpin-insertion model (Fig. 1*A*), a tether experiment confirmed that Bak α5 remains in the protein core. Because α5 lies beside α4 in the homology model of the Bak α2–α5 dimer (Fig. 2*E*, *Right*), just as in nonactivated Bak (Fig. 3*C*), we reasoned that Bak might still oligomerize if a disulfide link tethered α5 to α4. Bak with a cysteine in α5 (V142C) and either α4 (A107C) or the α3–α4 loop (P102C) (Fig. 3*C*) retained apoptotic function (Fig. S1*A*). Induced oxidation tethered the introduced cysteines, whether Bak was activated or not (Fig. 3*D*). Notably, these tethers did not block tBid-induced cytochrome *c* release (Fig. 3*E*), whereas a tether in wild-type Bak linking C14 to C166 did.

Finally, mutagenesis of Bak has strongly implicated several α5 residues, including G126, V129, and F134, in formation of the BH3:groove dimer (7). Additionally, by analogy to Bax, Bak α5 residues R127, A130 and F134 make important contacts with conserved BH3 residues within that dimer (10). Hence, at least the N-terminal half of α5 is needed to maintain the α2–α5 dimer and therefore α5 cannot be surrounded by membrane (see *Discussion*).

In summary, the alternating IASD labeling of Bak α5 C-terminal residues, the labeling pattern of its groove residues, tether data that α5 and α4 remain a hairpin, and structural and mutational data that α5 is required to form the dimers that join to make the oligomers, all suggest that α5 of oligomeric Bak is

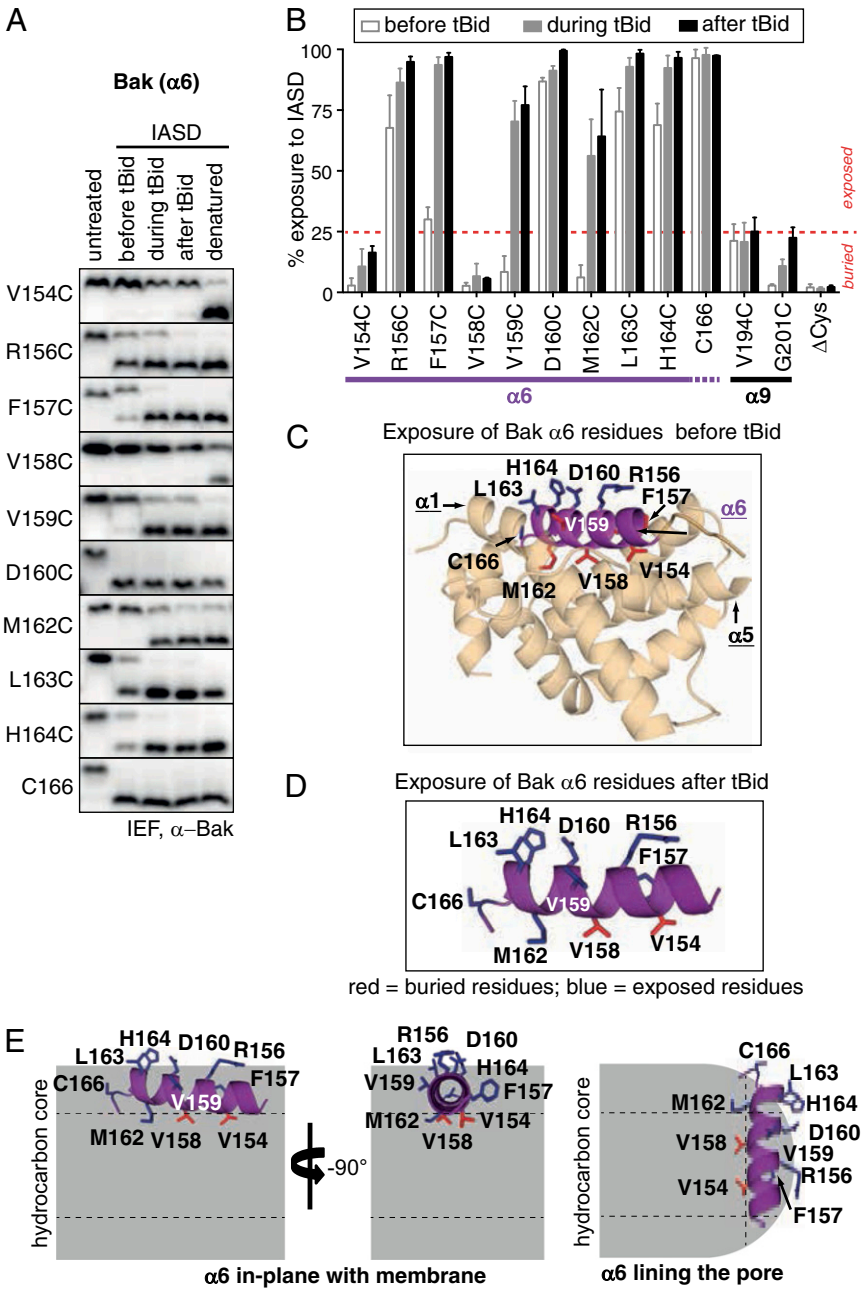

Fig. 4. Bak α6 exhibits no hallmarks of a TM domain. (*A*) IASD labeling of Bak α6 residues. Data are representative of two or more independent experiments. (*B*) Quantified IASD labeling of α6. Data are mean ± SD ($n = 3$) or range ($n = 2$ for D160, C166, G201C, ΔCys). (*C* and *D*) Only one face of Bak α6 is buried before and after tBid. The location of exposed (blue) and buried (red) α6 cysteine residues before (*C*) and after (*D*) tBid treatment is shown on the structure of nonactivated Bak. See also Fig. S4. (*E*) Diagrams of α6 in-plane with the MOM, including lining the pore. The side-chains of α6 residues are indicated as exposed (blue) or buried (red). The hydrocarbon core of the membrane (gray) is ~30 Å thick, and dotted lines indicate the depth (7.5 Å) to which IASD can penetrate from both sides of the membrane (31).

sandwiched between the membrane and a BH3:groove interface, as in the in-plane model (Fig. 2*E*), and not fully surrounded by the MOM, as in the hairpin insertion model (Fig. S3*B*).

Bak α6 Exhibits No Hallmarks of a TM domain. The nine Bak α6 residues tested (Fig. 4 *A* and *B* and Fig. S4*A*) all retained function (Fig. S1*A* and Table S2). Their labeling before tBid was consistent with the structure of nonactivated Bak, which shows one side of α6 on the protein surface and the other buried in its interior (Fig. 4*C*). Remarkably, however, after tBid treatment only two tested α6 residues (V154C and V158C) remained buried (Fig. 4*D*). This high proportion of exposed residues (seven of nine) argues strongly against α6 forming a TM domain (i.e., one fully surrounded by the lipid bilayer). The increased exposure of α6 residues (Fig. 4 *A* and *B* and Fig. S4*A*) suggests instead that this highly amphipathic helix lies in-plane with the membrane, either facing the cytosol or lining a pore (Fig. 4*E*) (see *Discussion*). In either case, two residues on one face of α6 become buried in the MOM, whereas those on its other face remain exposed or become more exposed.

A Detergent Test Confirms α5 of Oligomeric Bak Lies Within Protein Structure. To further test our inference above that some α5 residues not labeled by IASD in oligomeric Bak are buried within

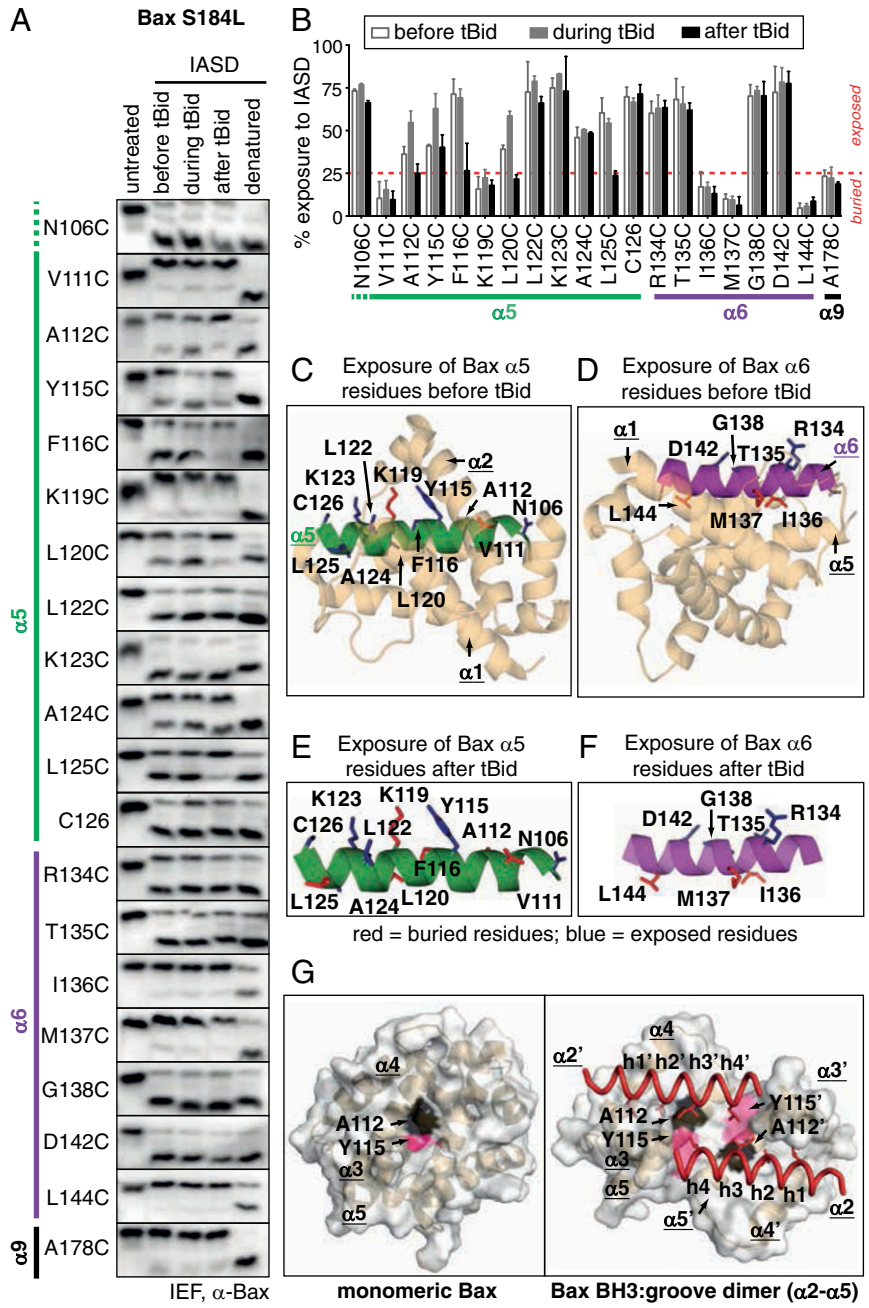

Fig. 5. Many α5 and α6 residues in oligomeric Bax S184L are accessible to IASD. (*A*) IASD labeling of BaxS184L cysteine variants. The mitochondrial membranes, washed to remove peripherally attached protein, were incubated with tBid and IASD as in Fig. 1*B*. Data are representative of two or more independent experiments. (*B*) Quantified IASD labeling. Data are mean ± SD ($n = 3$) or range ($n = 2$ for N106C, L120C, K123C, M137C, L144C). (*C–F*) Location of exposed and buried residues before and after tBid. The structure of nonactivated Bax (PDB ID code 1F16) is used to demonstrate the location of exposed (blue) and buried (red) cysteine residues before and after tBid treatment. See also Fig. S6. (*G*) A central region of Bax α5, including A112 and Y115, participates in the BH3-binding groove. A112 (black) and Y115 (pink) are shown on a surface representation of nonactivated monomeric Bax (5) (*Left*, 1F16 with α9 removed) and a model of the Bax BH3:groove dimer based on the Bax crystal structure (10) (*Right*, PDB ID code 4BDU). In the dimer, the two α2 helices (red tubes), and the h1-h4 BH3 residues (red side-chains), which make key hydrophobic groove contacts, are indicated. In the groove of nonactivated cytosolic Bax, α9 (not shown) will limit access of IASD to A112 and Y115 just as α2 does in the dimer.

protein structure (i.e., the α2–α5 dimer, rather than the MOM), we compared their labeling before and after treatment with the detergent 3-[(3-cholamidopropyl)dimethylammonio]-1-propanesulfonate (CHAPS), which frees Bak and Bax from the membrane but is thought not to significantly affect their structures. As expected, CHAPS exposed both α9 residues tested and the two α6 residues buried in oligomeric Bak (Fig. S4 *B* and *C*). In α5, CHAPS exposed Y143C fully, and V142C and L132C to some extent, but V129C, L131C, and G133C remained unlabeled, consistent with their burial in protein structure rather than the MOM. Thus, the membrane topologies of α5 and α6 differ: whereas α5 remains in the protein core, with only one face buried in the MOM, α6 seems to lie on the membrane surface or line a pore (see *Discussion*).

In Oligomeric Bax and Bax S184L, Many α5 and α6 Residues Are Exposed to IASD. Because our results for α5 and α6 in oligomeric Bak were inconsistent with the hairpin insertion model proposed for Bax (20),

we reexamined Bax topology. To facilitate comparison with Bak, we made most cysteine substitutions in a Bax variant targeted to the mitochondria (BaxS184L) (32, 33), so that tBid treatment of membrane fractions could efficiently activate most Bax molecules. Eighteen of the BaxS184L cysteine substitutions in α5 or α6 were functional and suitable for analysis (Fig. S1*C* and Tables S1 and S2). Pilot experiments revealed that some BaxS184L was only peripherally associated with the MOM, but an added incubation-wash step removed this population, leaving only fully activated oligomeric Bax (Fig. S5*A*).

Without tBid treatment, only two of the 18 Bax α5 residues tested (V111C and K119C) were "buried" as assessed by <25% IASD labeling, although three others (A112C, Y115C, L120C) in the middle of α5 were labeled only modestly (<40%) (Fig. 5 *A* and *B*). This pattern is consistent with the nonactivated Bax structure (PDB ID code 1F16) (5), in which other helices surround the middle of α5, whereas its C terminus is exposed (Fig. 5*C*). Labeling of Bax α6 before tBid was also consistent with that structure, as the three unlabeled residues (I136C, M137C, L144C) face the Bax interior (Fig. 5 *A*, *B*, and *D*).

After tBid treatment, V111C and K119C remained buried, but most central Bax α5 residues, like those in Bak, were modestly labeled (Fig. 5 *A* and *B*). Notably, Y115C remained 40% exposed, significantly more than the α9 residues ($P < 0.01$). Therefore, the unlabeled stretch in α5 is unlikely to be longer than six residues (F116 to V121), arguing strongly against Bax α5 as a TM domain.

Pertinently, three other central Bax α5 residues (A112C, Y115C, L120C) were labeled most during tBid treatment (Fig. 5 *A* and *B*), reflecting transient exposure. Because at least two of them (A112C and Y115C) line the open hydrophobic groove (Fig. 5*G*, *Left*), their transient exposure suggests that tBid uncovers the BaxS184L groove, but these residues are then reburied in the BH3:groove dimers by insertion of the Bax BH3 (Fig. 5*G*, *Right*). Notably, formation of the BH3:groove dimer relies on residues within the conserved N-terminal half of Bax α5, including R109, A112, and F116, which contact critical BH3 residues (10). Moreover, after tBid treatment, the α5 C terminus had a periodic labeling pattern, like that in Bak: the last five residues exhibited exposure (L122C/K123C), then partial/full burial (A124C/L125C), and then full exposure again (C126) (Fig. 5 *A*, *B*, and *E*, and Fig. S6*A*). Thus, the labeling pattern of Bax α5 supports the in-plane model (Fig. S6*B*) but not the hairpin insertion model (Fig. S6*C*).

After tBid treatment, we found no evidence that Bax α6 formed a TM domain, as residues throughout α6 were exposed (Fig. 5 *A*, *B*, and *F*). Instead, the helix appeared two-sided, with one side exposed (R134C, T135C, G138C, D142C) and the other buried (I136C, M137C, L144C), consistent with α6 lying in plane with the bilayer or lining a pore (Fig. S6 *B* and *C*).

We also assessed substitutions in α5 or α6 of wild-type Bax following induction of apoptosis in cells by etoposide (Figs. S1*D* and S5 *B*–*E*, and Tables S1 and S2), which provoked Bax oligomerization and cytochrome *c* release (Fig. S5 *B* and *C*). We compared Bax in the membrane fraction with nonactivated Bax in the cytosol of untreated cells. Significantly, all five α5 or α6 residues tested were exposed to IASD in oligomeric Bax, and Bax in etoposide-treated cells labeled similarly to BaxS184L activated by tBid (Fig. 5*B* and Fig. S5*E*).

Thus, many α5 and α6 residues in oligomeric Bax were exposed to IASD, arguing strongly against α5 and α6 spanning the MOM as a TM hairpin. The data are instead consistent with α5 and α6 lying on the membrane surface, with α5 within a BH3:groove dimer, partly covered by other core helices (e.g., α2–α4) (10), as in the in-plane model (Fig. S6*B*).

Low Salt Buffer Reduces IASD Labeling of Certain Bak and Bax Residues. We then addressed why a previous Bax topology study reported burial of α5 and α6 in the MOM of etoposide-treated cells (20). We noted that their IASD-labeling buffer had negligible salt (only 2 mM $MgCl_2$), whereas ours had a more physiological level (2.5 mM $MgCl_2$, 100 mM KCl). Therefore, we compared labeling for six substitutions within wild-type Bax in the cytosolic and membrane fractions using our medium salt buffer or buffers having either no added salt or only 2 mM $MgCl_2$.

Surprisingly, all five α5 and α6 residues tested in low salt (either 2 mM $MgCl_2$ or none) labeled less in membrane-associated Bax than cytosolic Bax ($P < 0.05$ for each) (Fig. 6). Significantly, in buffer A [that used by Annis et al. (20)], these residues were labeled 62–88% in the cytosol but only 19–47% in mitochondria. In the prior work, lower labeling in mitochondrial than cytosolic Bax was reasonably attributed to insertion of the residue into the MOM (20). However, in our medium salt buffer, IASD labeled

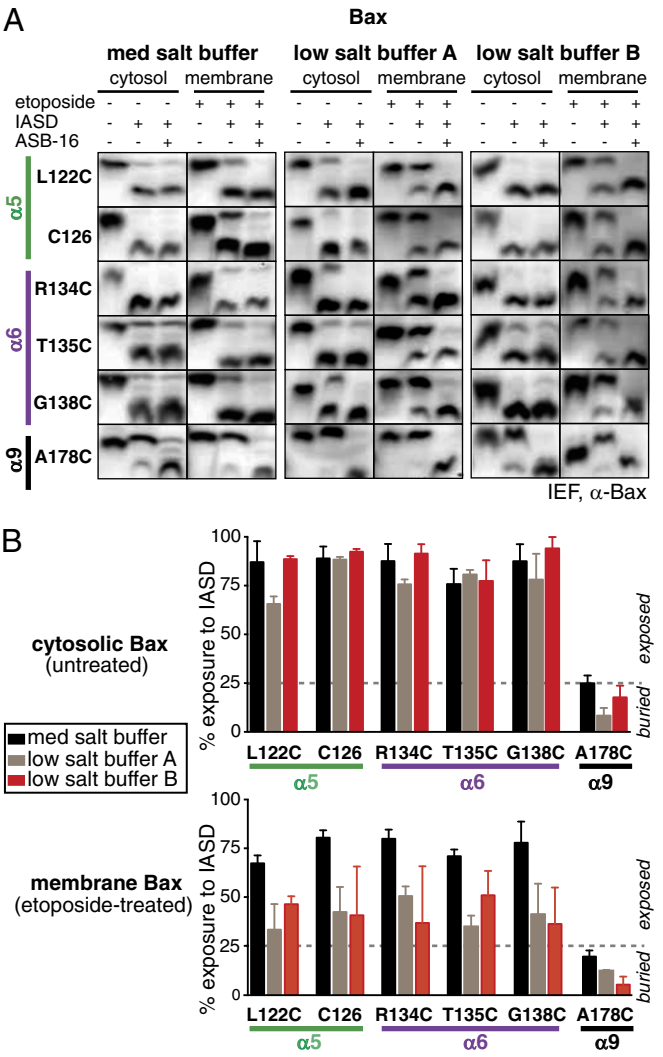

Fig. 6. Low salt buffers reduce IASD labeling of certain Bax residues. (*A*) Bax that translocates to mitochondria after etoposide is labeled less in low salt buffers. $Bak^{-/-}Bax^{-/-}$ MEFs stably expressing the Bax cysteine substitutions were left untreated or incubated with etoposide to induce apoptosis, and their cytosol and membrane fractions analyzed in low or medium salt buffers, as indicated. Data are representative of three independent experiments. Low salt buffer A is that used by Annis et al. (20). (*B*) Quantified IASD labeling shows that the reduced labeling in low salt is confined to membrane-bound Bax. The cytosolic Bax was untreated (*Upper*), whereas the membrane-bound Bax came from etoposide-treated cells (*Lower*). Data are mean ± SD ($n = 3$). Fig. S7*A* shows overlays of low and medium salt IASD data on all of the Bak and BaxS184L variants, before, during and after tBid treatment. IASD labeling of Bak residues from etoposide-treated cells in low salt closely resembled that produced by tBid (Fig. S7*B*).

the membrane-associated and cytosolic Bax comparably (P = not significant), with all five α5 or α6 residues exposed 68–95% (Fig. 6). Why low salt did not alter labeling of residues in cytosolic Bax is unclear. Perhaps the cytosolic fraction contains enough residual intracellular salt (the cytoplasm is 140 mM in K^+ equivalents) to enhance IASD labeling.

Analysis of all our cysteine substitutions of Bak and BaxS184L revealed that although several residues (~8 of 39) were labeled substantially less in low than medium salt after tBid, the pattern for most α5 and α6 residues closely resembled that in medium salt (Fig. S7*A*). For example, after tBid the α5 C terminus and α6 of both Bak and BaxS184L showed periodic labeling (sidedness). Thus, both large series of IASD-labeling experiments support the in-plane model.

Discussion

How oligomerization of Bak or Bax disrupts MOM integrity, the "point of no return" in apoptosis, remains unknown. The structural similarity of globular Bcl-2 family members to certain bacterial toxins prompted the longstanding view that Bak and Bax, in analogy to those toxins, initiate pore formation by inserting α5 and α6 as a hairpin through the MOM (13). In seeming accord, several cysteine substitutions in Bax α5 and α6 became less accessible to IASD after an apoptotic stimulus (20). The proposal that Bak and Bax become multispanning membrane proteins early in apoptosis has been widely embraced, and α5 and α6 are often designated as their "pore-forming domain" (e.g., ref. 17).

Several lines of evidence presented here establish that neither α5 nor α6 becomes surrounded by the bilayer in the oligomers, as in the hairpin insertion models (Fig. 7*A*, variant 1 or 2). First, in TM helices, the membrane protects a central segment of at least 10–12 residues from IASD (30, 31), but the α6 helices of Bak and Bax displayed no substantial protected region, and the fully protected stretch might span at most nine residues in Bak α5 (Fig. 2) and six in Bax α5 (Fig. 5). Instead, our results, summarized in Fig. 7*B*, indicate that α5 and α6 of both proteins are only shallowly inserted. Second, we show that the central segment of Bak α5 remains part of the BH3:groove dimer (Fig. 3) (7), as suggested by a crystal structure for Bax (10) and very recently for Bak as well (34). Accordingly, Bak with α5 tethered to α4 could still be activated to release cytochrome *c* (Fig. 3 *C*–*E*), and CHAPS did not expose several α5 residues in activated Bak to IASD (Fig. S5 *B* and *C*). Moreover, the alternating pattern of IASD labeling near the α5 C-termini of both Bak and Bax is consistent with an in-plane helix rather than a TM helix.

The multiple charged residues in α5 and α6 of Bak and Bax (Fig. 7*C*) also distinguish them from most TM domains (35). In their α6 helices, which are shorter than most TM helices (15 residues in Bak, 17 in Bax vs. a typical 20–25), Bak has two charged residues and Bax has six. The charged residues in α5 (two in Bak and three in Bax) most likely make salt bridges to maintain the BH3:groove dimer structure, like the conserved Arg near the α5 N terminus (Fig. 7*C*), which binds the invariant BH3 Asp.

Finally, the hairpin insertion model appears incompatible with the BH3:groove α2–α5 dimer, which represents a crucial element in the oligomers (2, 4). Much of α5, particularly its N-terminal half, is nearly identical in Bak and Bax (Fig. 7*C*), and mutagenesis and structural data strongly implicate a number of these residues in forming the BH3:groove symmetric dimer. As well as the ion pair made by the

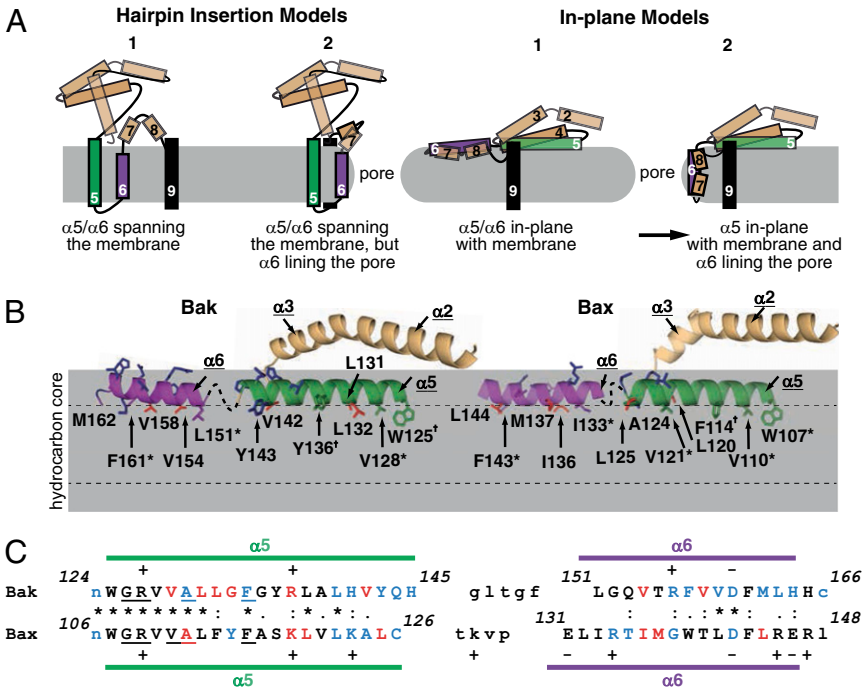

Fig. 7. To form apoptotic pores, Bak and Bax insert helices α5 and α6 in-plane into the MOM. (*A*) Four possible membrane topologies for activated Bak and Bax. In the hairpin insertion models, α5 and α6 dissociate from the hydrophobic protein core and insert across the MOM as a hairpin, either with both helices spanning the membrane as TM domains (variant 1), or with the α6 polar face lining the apoptotic pore (variant 2). In the in-plane models, α5 remains with α2–α4 in the core, where it contributes one face to a BH3:groove interface and the opposite to the membrane, whereas α6 disassociates from the α2–α5 core and collapses onto the membrane, presenting its polar face to the cytosol and its nonpolar face to the membrane (variant 1). Several of the in-plane helices may then slide into a nascent pore to promote its development or stabilize its wall (variant 2). (*B*) Burial of the nonpolar faces of α5 and α6 in the MOM indicated by IASD labeling. Cartoon representations of α6 connected to a monomer (α2, α3, α5) from models of the Bak and Bax BH3:groove dimers (see *SI Materials and Methods* for details of dimer models). The immersion of α5 and α6 into the MOM is based on evidence that the IASD alkylating group can label cysteines 7.5 Å (dotted line) into the hydrophobic aliphatic region (gray, ~30 Å), whereas its charged sulfonates lie in the head-group regions (31). Side-chains are shown for several residues that were exposed (blue) or buried (red), or were not tested because of loss-of-function (†) or other (*) reasons (green or purple) (Tables S1 and S2). (*C*) Sequence comparison of Bak and Bax across their α5/α6 regions, highlighting residues that were exposed (blue) or buried (red) after activation of Bak and Bax. Residues that are identical (*), conserved (:), semiconserved (.), or charged (+ or –) are indicated. Conserved residues in α5 with key roles in formation of the BH3:groove dimer are underlined.

N-terminal Arg, Bax V111, A112, and F116 help line the hydrophobic pockets into which the key hydrophobic BH3 residues at h4, h3, and h2 protrude, respectively (10). The equivalent Bak residues most likely have the same function (2, 34, 36) and many other α5 residues in both proteins must make contacts with α4 and the second α5 helix in their compact stable α2–α5 dimers (2, 10, 34).

Three factors may help to explain why Annis et al. (20) reached the conclusion that α5 and α6 of Bax insert into membranes as a hairpin. First, only two residues in α5 and three in α6 were examined, too few to clearly discriminate between a transmembrane helix like α9 and a helix laying along the membrane surface and inserting only one face into the MOM, as we suggest for α5 and α6. Second, we unexpectedly found that the low salt concentration they used for IASD labeling led to lower labeling of some residues in mitochondrial Bax than cytosolic Bax (Fig. 6). Finally, whereas the Bak and Bax we studied were fully functional and formed oligomers, Annis et al. focused mainly on a unique *myc*$^{-/-}$ rat cell line in which etoposide evokes some Bax translocation to mitochondria but, for unknown reasons, Bax remains monomeric, does not promote cytochrome *c* release or apoptosis (20), or even display the 6A7 activation marker (37). In their cells constitutively reexpressing Myc, where etoposide did evoke Bax oligomerization, only one α5 and three α6 residues were tested, and the two judged to be buried (L122C and R134C) were clearly exposed in our study (Figs. 5 *A* and *B* and 6).

Very recently, another study reported IASD labeling results on Bak (38). That study used a buffer system similar to ours but used transiently transfected Bak cDNA rather than stable transfection followed by apoptotic signaling. Because the labeling varied with the amount of Bak cDNA, it is difficult to compare their results with ours, but the increased labeling of the one α5 and two α6 residues they tested in cells exposed to a lethal amount of Bak cDNA appears inconsistent with the hairpin model.

A recent detailed EPR study on tBid-activated Bak in large unilamellar vesicles (27) concluded that α5 remains associated with α2–α4 in the protein core, whereas α6 separates from the core, and shallowly inserts into the membrane (21). This biophysical approach with a molecularly defined system also strongly argues against the hairpin insertion model and supports the in-plane model.

Our evidence against α5 spanning the MOM argues against both variants of the hairpin insertion model (Fig. 7*A*). Further evidence against them is that α5 and α6 appear to separate at an early stage of activation of Bax (10) and Bak (27, 34), as in the in-plane models 1 and 2 (Fig. 7*A*). Indeed, their function appears to require that α5 and α6 separate, because tethering α5 to α6 in either blocked release of cytochrome *c* (10, 34). Instead, α5 remains within the α2–α5 core, because α4–α5 hairpins remain in the α2–α5 core dimer structure of both proteins (Fig. 2*E* and Fig. S6*B*), and an α4–α5 tether did not block function of either Bax (10) or Bak (Fig. 3 *C*–*E*).

Thus, structural, biophysical, and biochemical data now all strongly suggest that, during pore formation, neither α5 nor α6 insert across the MOM as TM domains, and that α5 remains with α2–α4 in the core, whereas α6 separates from the core and shallowly inserts into the membrane.

The structural and biophysical data and our IASD labeling results fit best with a model in which both α5 and α6 lie on the membrane surface: the in-plane model (Fig. 7 *A* and *B*). Helix 5 is proposed to contact the membrane via a bent planar surface, comprising two α4–α5 hairpins, that is rich in aromatic and other hydrophobic residues, as shown by the α2–α5 dimer structure of Bax (10) and now also of Bak (34). An in-plane topology for α5 of both Bak and Bax is supported by the two-sidedness of its C-terminal region: after tBid treatment its polar face is exposed and its nonpolar face buried, and equivalent residues (Bak Y143C and Bax L125C) make the transition to burial. The two-sided labeling pattern of α6 in oligomeric Bak and Bax is also indicative of an in-plane helix, as is the shallow insertion of α6 revealed by EPR studies of Bid-activated Bak (21).

Localization of α5 and α6 to the membrane surface suggests that oligomeric Bak and Bax may not permeabilize the MOM by forming a single well-defined pore entirely bounded by protein. It fits better with the hypothesis that the oligomers impose tension and strain on the bilayer, leading to pores partially bounded by lipid (23, 25). Mass introduced into the bilayer outer leaflet by hydrophobic side-chains of residues in α4, α5, and α6 (and possibly also α7 and α8) will impose tension and positive curvature on the bilayer (15), and the angle between the two α4–α5 hairpins in the α2–α5 core dimers of both proteins (10, 34) might well exacerbate the tension. As the oligomers increase in size, the strain is expected to provoke nearby fusion of the outer and inner leaflets, nucleating a proteolipidic pore (15).

The oligomerization of Bak and Bax may be enhanced not only by protein–protein interactions but also by dimers sinking further into the hydrophobic membrane core. Because lipidic pores tend to be metastable (25), we suggest that stable pores will result when oligomers corral the imposed surface tension within focused regions by forming circles of variable size. In the oligomers, our results suggest that only α9 represents a conventional TM domain, but an appealing feature of the in-plane model is that several of their other helices, possibly including α4 to α8, could readily slide into a nascent pore to line its wall and thereby to stabilize the pore (in-plane variant 2) (Fig. 7*A*). Within the oligomers, multiple helices of Bak and Bax may thus both drive formation of the pores and help to maintain them.

Materials and Methods

Cloning and Expression of Bak and Bax Variants. Single cysteines were introduced into human BakΔCys (C14S/C166S), human BaxΔCys (C62S/C126S), or BaxS184LΔCys by overlap extension PCR and cloned into the pMX-IG (IRES-GFP) retroviral vector. The variants were then stably expressed in SV40-immortalized *Bak*$^{-/-}$*Bax*$^{-/-}$ MEFs, as described previously (7). Each cell line was generated by retroviral infection at least twice, with cells maintained in culture for less than 3 wk.

Preparation of Subcellular Fractions. The MEFs stably expressing Bak and Bax variants were used to generate cytosol and membrane fractions (enriched for mitochondria) as previously described (7). Briefly, cells were suspended at 1×10^7 cells/mL in medium salt buffer (100 mM sucrose, 20 mM Hepes-KOH pH 7.5, 100 mM KCl, 2.5 mM $MgCl_2$) supplemented with Complete protease inhibitors (Roche), 4 μg/mL pepstatin A (Sigma-Aldrich), and 0.025% digitonin (wt/vol) (Calbiochem, Merk). After 10 min on ice, the permeabilized cells were centrifuged at 13,000 × *g* for 5 min to generate the cytosol fraction and the pellets were resuspended in buffer lacking digitonin to generate the membrane fraction. Where indicated, medium salt buffer was replaced with a buffer without added salt (low salt buffer B: 300 mM sucrose, 10 mM Tris·HCl pH 7.4, 1 mM EDTA) or one containing 2 mM $MgCl_2$ (low salt buffer A: 250 mM sucrose, 20 mM Hepes-KOH pH 7.5, 1 mM EDTA, 2 mM $MgCl_2$) (20).

To remove peripherally attached Bax and BaxS184L, membrane fractions were incubated for 15 min at room temperature, centrifuged, and resuspended in the same buffers lacking digitonin.

Activation of Bak and Bax by tBid or Etoposide. To activate Bak and BaxS184L and permeabilize mitochondria, membrane fractions from cells expressing these proteins were incubated with 100 nM tBid [truncated human Bid cleaved by caspase-8 for 30 min at 30 °C (7)]. To induce apoptosis, cells were incubated with 10 μM etoposide (Sigma-Aldrich) for 24 h. Apoptosis was assessed by uptake of propidium iodide (5 μg/mL) by flow cytometry (FACScan, BD Biosciences). Where indicated, caspases were inhibited by addition of 50 μM caspase inhibitor Q-VD.OPh (MP Biomedicals).

Cysteine Accessibility to IASD Labeling. To test whether each cysteine substituted in Bak or Bax was in a hydrophobic environment, cytosol or membrane fractions were incubated with 10 mM IASD (Molecular Probes) for 30 min at 30 °C. The five samples for IEF were each incubated for a total of 60 min at 30 °C. IASD was added at 30 min in four of the samples (omitted for the negative control). tBid was added to two of the samples: at 30 min for the "during tBid" samples so that IASD was present during tBid activation of Bak/Bax; or at 0 min for the "after tBid" samples so that IASD was present only after pore formation. For the "denatured" samples, untreated membrane fractions were solubilized with 1% ASB-16 for 10 min at room tem-

perature before IASD labeling. Labeling was quenched by adding 200 mM DTT and samples solubilized with 1% (wt/vol) ASB-16 (Calbiochem) for 10 min at room temperature. After centrifugation at 13,000 × *g* for 5 min, supernatants were combined with an equal volume of IEF sample buffer [7 M urea, 2 M thiourea, 2% (wt/vol) CHAPS, complete protease inhibitors, 4 μg/mL pepstatin A, 1% ASB-16, and 0.04% bromophenol blue] and loaded immediately onto Novex pH 3–7 IEF gels (Life Technologies). BaxS184L and Bax variants were labeled similarly, but peripherally attached protein was first removed from the membrane fractions by an incubation-wash step, and IEF focusing was improved by increasing the final ASB-16 to 2% (wt/vol).

One-Dimensional Isoelectric Focusing and IASD Quantification. One-dimensional IEF was performed as described previously (39). Briefly, gels were focused with increasing voltage (100 V, 200 V, and 500 V for 1 h each) using a EV265 power pack (Consort). The gels were then soaked in SDS buffer [75 mM Tris·HCl pH 6.8, 15% (vol/vol) glycerol, 0.6% SDS] for 5 min before transfer to PVDF membranes at 40 mA for 2.5 h, followed by immunoblotting.

To quantify IASD labeling, chemi-luminescent signals were detected using the ChemiDoc XRS+ System (Bio-Rad) and analyzed with Image Lab 3.0 (Bio-Rad). Within each lane, rectangles of equal dimensions were placed over the unlabeled and labeled bands, and pixels counted digitally, background subtracted and percent labeling calculated. Data are represented as mean ± SD ($n = 3$) or range ($n = 2$), as indicated in legends and in Tables S1 and S2. For comparison of means, an unpaired two-tailed Student *t* test was applied with a *P* value significance of <0.05.

Additional Information. See *SI Materials and Methods* for Blue Native/PAGE and gel-shift assays, SDS/PAGE and immunoblotting, and structural modeling.

ACKNOWLEDGMENTS. We thank T. Kratina for technical support; N. Church, J.-G. Zhang, R. Uren, C. Hockings, and M. Ritchie for advice on isoelectric focusing and statistics; P. Colman for comments on the manuscript; and T. Kitamura for the pMX-IG vector. This work was supported in part by a Deutsche Forschungsgemeinschaft postdoctoral fellowship (to D.W.), the National Health and Medical Research Council (575559 and 1016701), the Australian Research Council (FT100100754 and FT100100791), the Leukemia and Lymphoma Society, the Victorian State Government Operational Infrastructure Support, and the Australian Government National Health and Medical Research Council Independent Research Institute Infrastructure Support Scheme.

1. Chipuk JE, Moldoveanu T, Llambi F, Parsons MJ, Green DR (2010) The BCL-2 family reunion. *Mol Cell* 37(3):299–310.
2. Czabotar PE, Lessene G, Strasser A, Adams JM (2014) Control of apoptosis by the BCL-2 protein family: Implications for physiology and therapy. *Nat Rev Mol Cell Biol* 15(1):49–63.
3. Bender T, Martinou JC (2013) Where killers meet—Permeabilization of the outer mitochondrial membrane during apoptosis. *Cold Spring Harb Perspect Biol* 5(1): a011106.
4. Westphal D, Kluck RM, Dewson G (2014) Building blocks of the apoptotic pore: How Bax and Bak are activated and oligomerize during apoptosis. *Cell Death Differ* 21(2):196–205.
5. Suzuki M, Youle RJ, Tjandra N (2000) Structure of Bax: Coregulation of dimer formation and intracellular localization. *Cell* 103(4):645–654.
6. Moldoveanu T, et al. (2006) The X-ray structure of a BAK homodimer reveals an inhibitory zinc binding site. *Mol Cell* 24(5):677–688.
7. Dewson G, et al. (2008) To trigger apoptosis, Bak exposes its BH3 domain and homodimerizes via BH3:groove interactions. *Mol Cell* 30(3):369–380.
8. Dewson G, et al. (2012) Bax dimerizes via a symmetric BH3:groove interface during apoptosis. *Cell Death Differ* 19(4):661–670.
9. Bleicken S, et al. (2010) Molecular details of Bax activation, oligomerization, and membrane insertion. *J Biol Chem* 285(9):6636–6647.
10. Czabotar PE, et al. (2013) Bax crystal structures reveal how BH3 domains activate Bax and nucleate its oligomerization to induce apoptosis. *Cell* 152(3):519–531.
11. Dewson G, et al. (2009) Bak activation for apoptosis involves oligomerization of dimers via their alpha6 helices. *Mol Cell* 36(4):696–703.
12. Ma S, et al. (2013) Assembly of the Bak apoptotic pore: A critical role for the Bak protein α6 helix in the multimerization of homodimers during apoptosis. *J Biol Chem* 288(36):26027–26038.
13. Muchmore SW, et al. (1996) X-ray and NMR structure of human Bcl-x_L, an inhibitor of programmed cell death. *Nature* 381(6580):335–341.
14. Parker MW, Feil SC (2005) Pore-forming protein toxins: From structure to function. *Prog Biophys Mol Biol* 88(1):91–142.
15. García-Sáez AJ (2012) The secrets of the Bcl-2 family. *Cell Death Differ* 19(11):1733–1740.
16. Antignani A, Youle RJ (2006) How do Bax and Bak lead to permeabilization of the outer mitochondrial membrane? *Curr Opin Cell Biol* 18(6):685–689.
17. García-Sáez AJ, et al. (2006) Peptides corresponding to helices 5 and 6 of Bax can independently form large lipid pores. *FEBS J* 273(5):971–981.
18. Qian S, Wang W, Yang L, Huang HW (2008) Structure of transmembrane pore induced by Bax-derived peptide: Evidence for lipidic pores. *Proc Natl Acad Sci USA* 105(45):17379–17383.
19. Fuertes G, et al. (2010) Pores formed by Baxα5 relax to a smaller size and keep at equilibrium. *Biophys J* 99(9):2917–2925.
20. Annis MG, et al. (2005) Bax forms multispanning monomers that oligomerize to permeabilize membranes during apoptosis. *EMBO J* 24(12):2096–2103.
21. Oh KJ, et al. (2010) Conformational changes in BAK, a pore-forming proapoptotic Bcl-2 family member, upon membrane insertion and direct evidence for the existence of BH3-BH3 contact interface in BAK homo-oligomers. *J Biol Chem* 285(37):28924–28937.
22. Martinez-Caballero S, et al. (2009) Assembly of the mitochondrial apoptosis-induced channel, MAC. *J Biol Chem* 284(18):12235–12245.
23. Terrones O, et al. (2004) Lipidic pore formation by the concerted action of proapoptotic BAX and tBID. *J Biol Chem* 279(29):30081–30091.
24. Kuwana T, et al. (2002) Bid, Bax, and lipids cooperate to form supramolecular openings in the outer mitochondrial membrane. *Cell* 111(3):331–342.
25. Bleicken S, Wagner C, García-Sáez AJ (2013) Mechanistic differences in the membrane activity of Bax and Bcl-xL correlate with their opposing roles in apoptosis. *Biophys J* 104(2):421–431.
26. Basañez G, et al. (1999) Bax, but not Bcl-x_L, decreases the lifetime of planar phospholipid bilayer membranes at subnanomolar concentrations. *Proc Natl Acad Sci USA* 96(10):5492–5497.
27. Aluvila S, et al. (2014) Organization of the mitochondrial apoptotic BAK pore: Oligomerization of the BAK homodimers. *J Biol Chem* 289(5):2537–2551.
28. Ferrer PE, Frederick P, Gulbis JM, Dewson G, Kluck RM (2012) Translocation of a Bak C-terminus mutant from cytosol to mitochondria to mediate cytochrome C release: Implications for Bak and Bax apoptotic function. *PLoS ONE* 7(3):e31510.
29. Zhu Q, Casey JR (2007) Topology of transmembrane proteins by scanning cysteine accessibility mutagenesis methodology. *Methods* 41(4):439–450.
30. Grziwa B, et al. (2003) The transmembrane domain of the amyloid precursor protein in microsomal membranes is on both sides shorter than predicted. *J Biol Chem* 278(9):6803–6808.
31. Grundling A, Blasi U, Young R (2000) Biochemical and genetic evidence for three transmembrane domains in the class I holin, lambda S. *J Biol Chem* 275(2):769–776.
32. Nechushtan A, Smith CL, Hsu YT, Youle RJ (1999) Conformation of the Bax C-terminus regulates subcellular location and cell death. *EMBO J* 18(9):2330–2341.
33. Fletcher JI, et al. (2008) Apoptosis is triggered when prosurvival Bcl-2 proteins cannot restrain Bax. *Proc Natl Acad Sci USA* 105(47):18081–18087.
34. Brouwer JM, et al. (2013) Bak core and latch domains separate during activation and freed core domains form symmetric homo-dimers. *Mol Cell*, 10.1016/j.molcel.2014.07.016.
35. Nilsson J, Persson B, von Heijne G (2005) Comparative analysis of amino acid distributions in integral membrane proteins from 107 genomes. *Proteins* 60(4):606–616.
36. Moldoveanu T, et al. (2013) BID-induced structural changes in BAK promote apoptosis. *Nat Struct Mol Biol* 20(5):589–597.
37. Soucie EL, et al. (2001) Myc potentiates apoptosis by stimulating Bax activity at the mitochondria. *Mol Cell Biol* 21(14):4725–4736.
38. Weber K, Harper N, Schwabe J, Cohen GM (2013) BIM-mediated membrane insertion of the BAK pore domain is an essential requirement for apoptosis. *Cell Reports* 5(2):409–420.
39. Tran VH, et al. (2013) Bak apoptotic function is not directly regulated by phosphorylation. *Cell Death Dis* 4:e452.